Positron Emission Tomography (PET)

Anatomic Imaging:

CT (Computed Tomography),
MRI (Magnetic Resonance Imaging)

Molecular Imaging:

SPECT (Single Photon Emission Computed Tomography)
PET (Positron Emission Tomography)

Oncology, Alzheimer's disease, Parkinson's disease

Beta-minus Decay

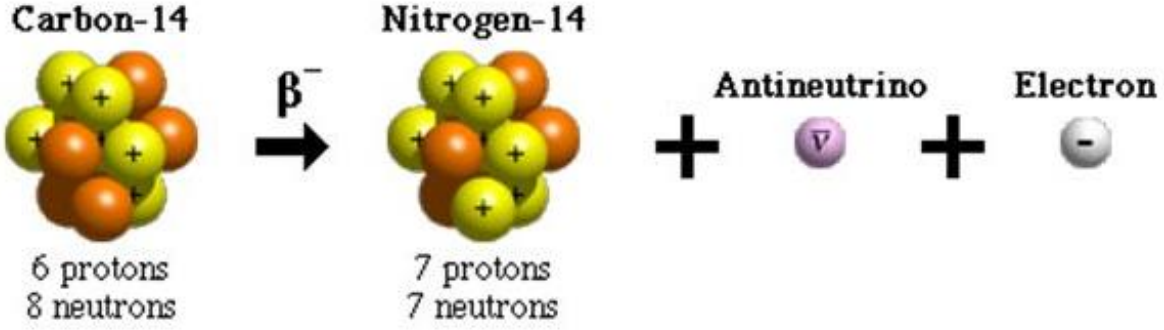

Beta-plus Decay

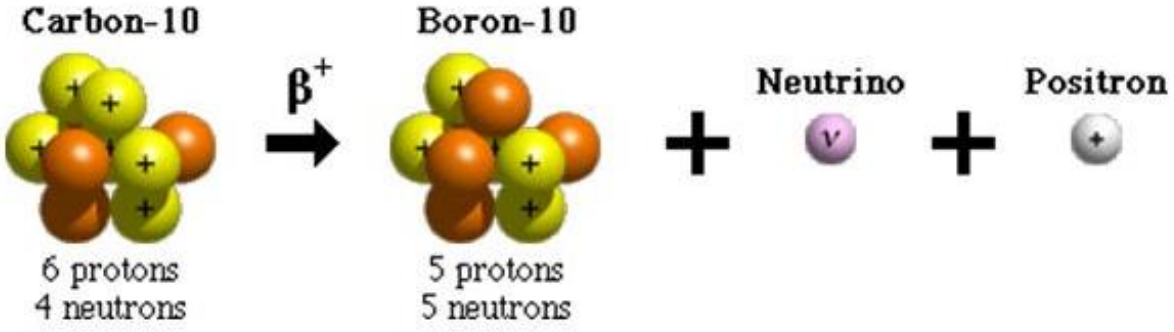

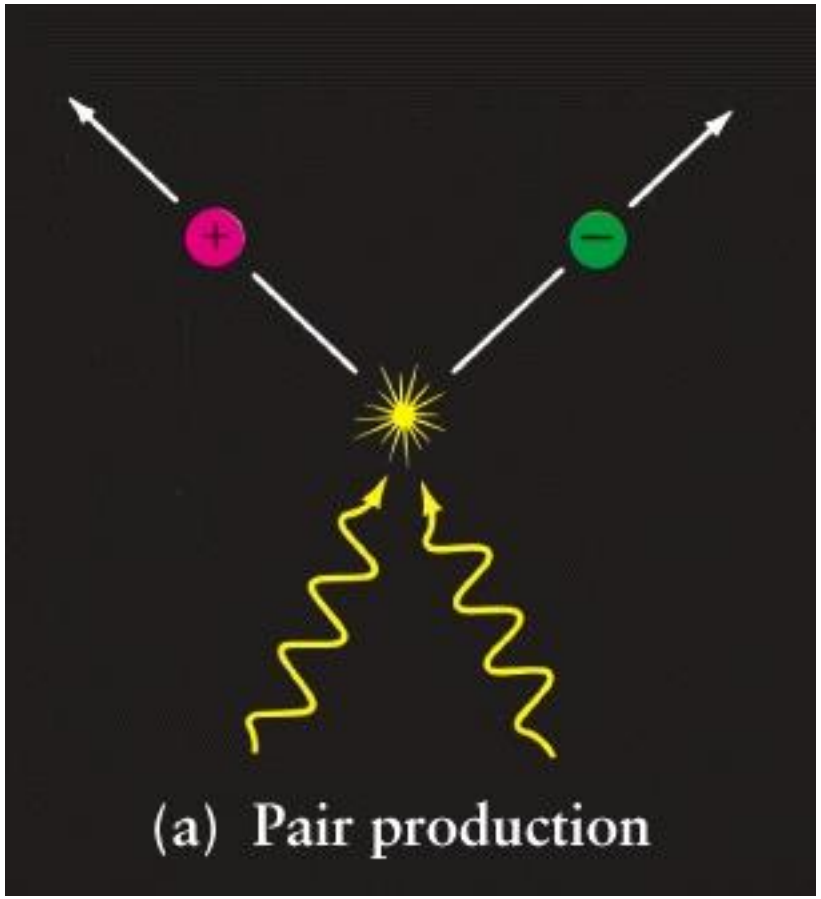
+
−
(a) Pair production

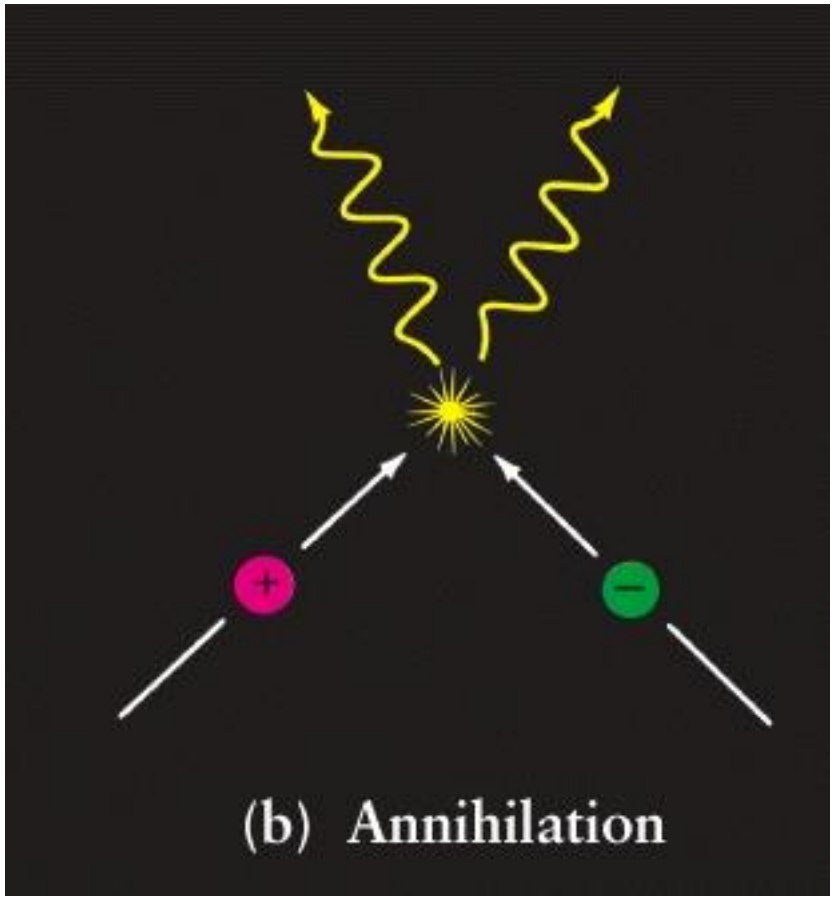
+
−
(b) Annihilation

FDG

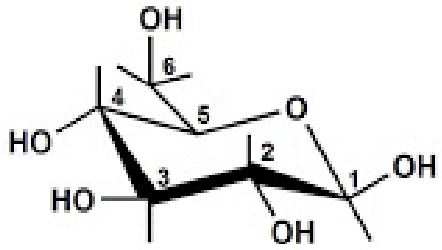

D-Glucose

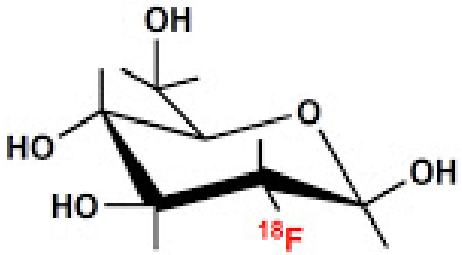

2-Fluoro-2-deoxy-D-glucose (FDG)

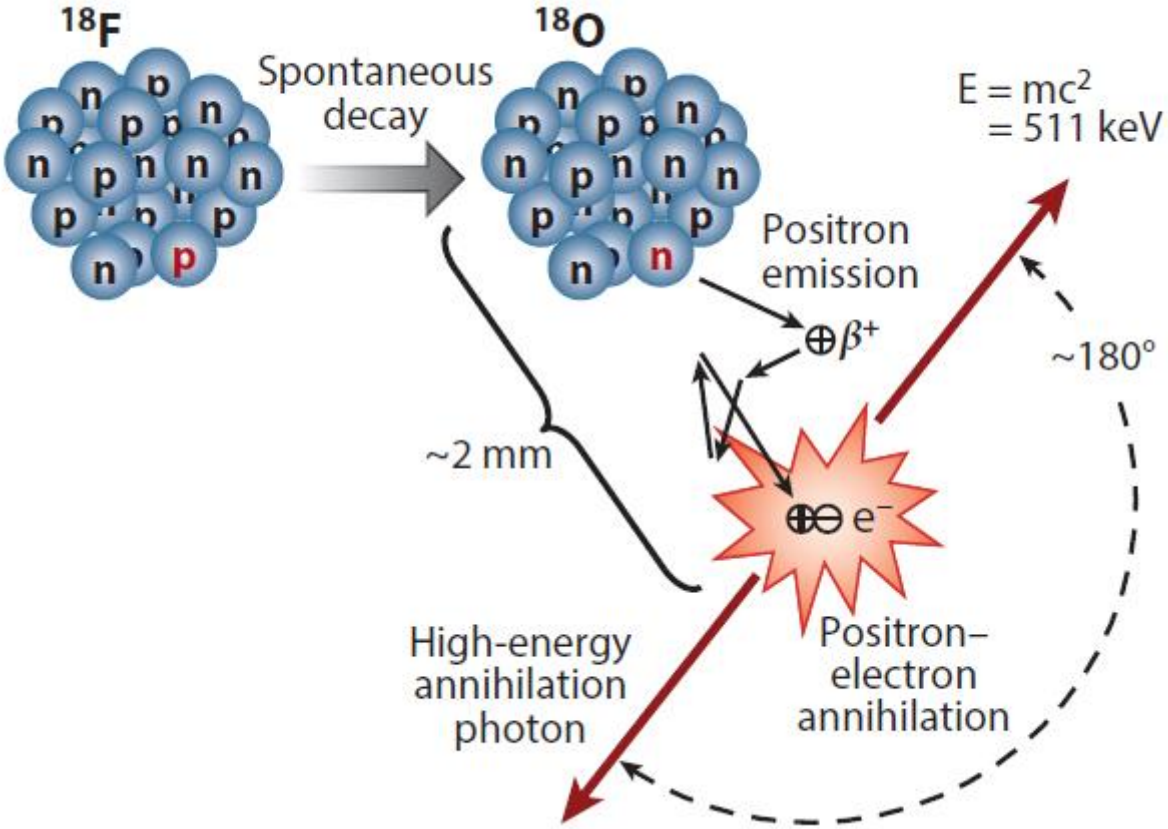
^{18}F
^{18}O
Spontaneous decay
E = mc^2
= 511 keV
Positron emission
β^+
~180°
~2 mm
e$^-$
High-energy annihilation photon
Positron–electron annihilation

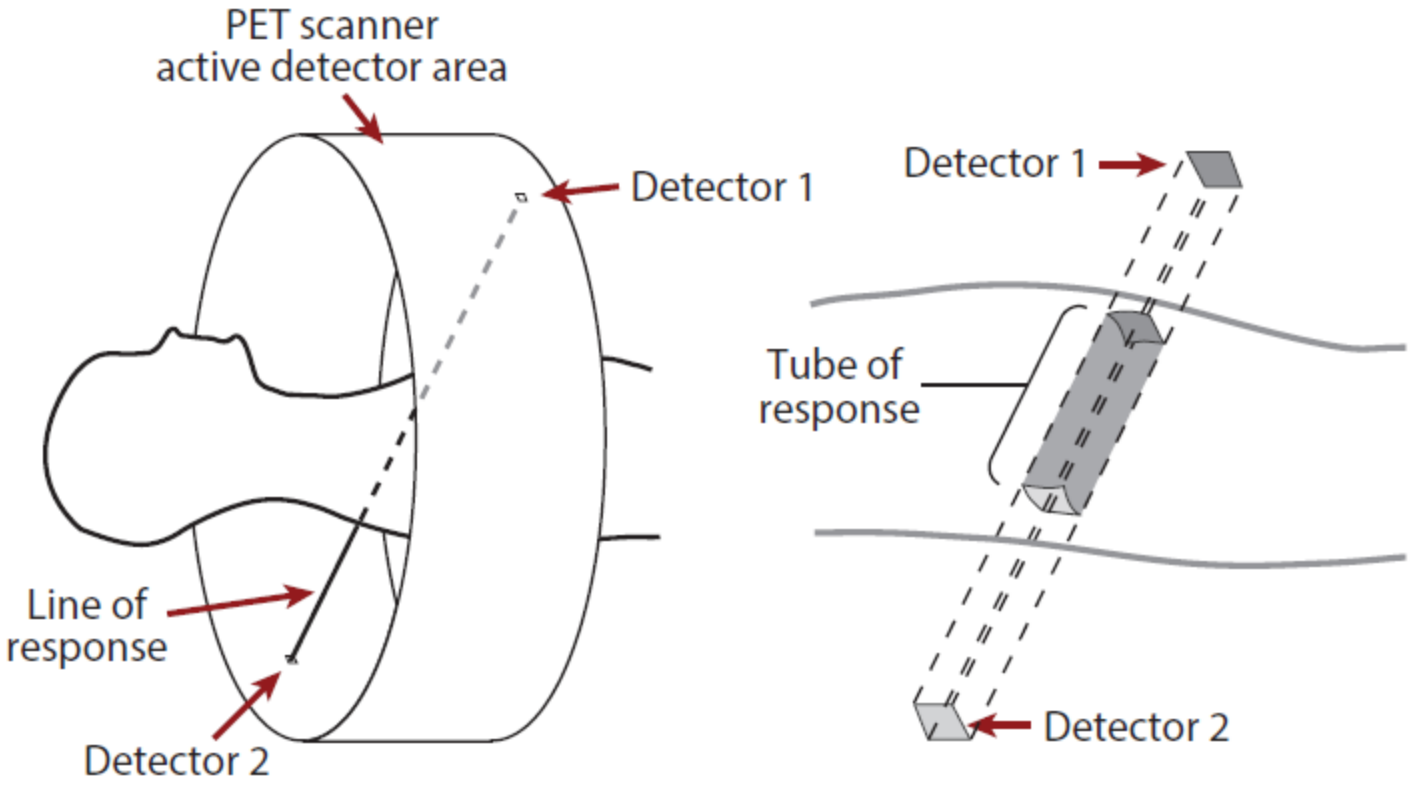
PET scanner
active detector area
Detector 1
Line of
response
Detector 2
Detector 1
Tube of
response
Detector 2

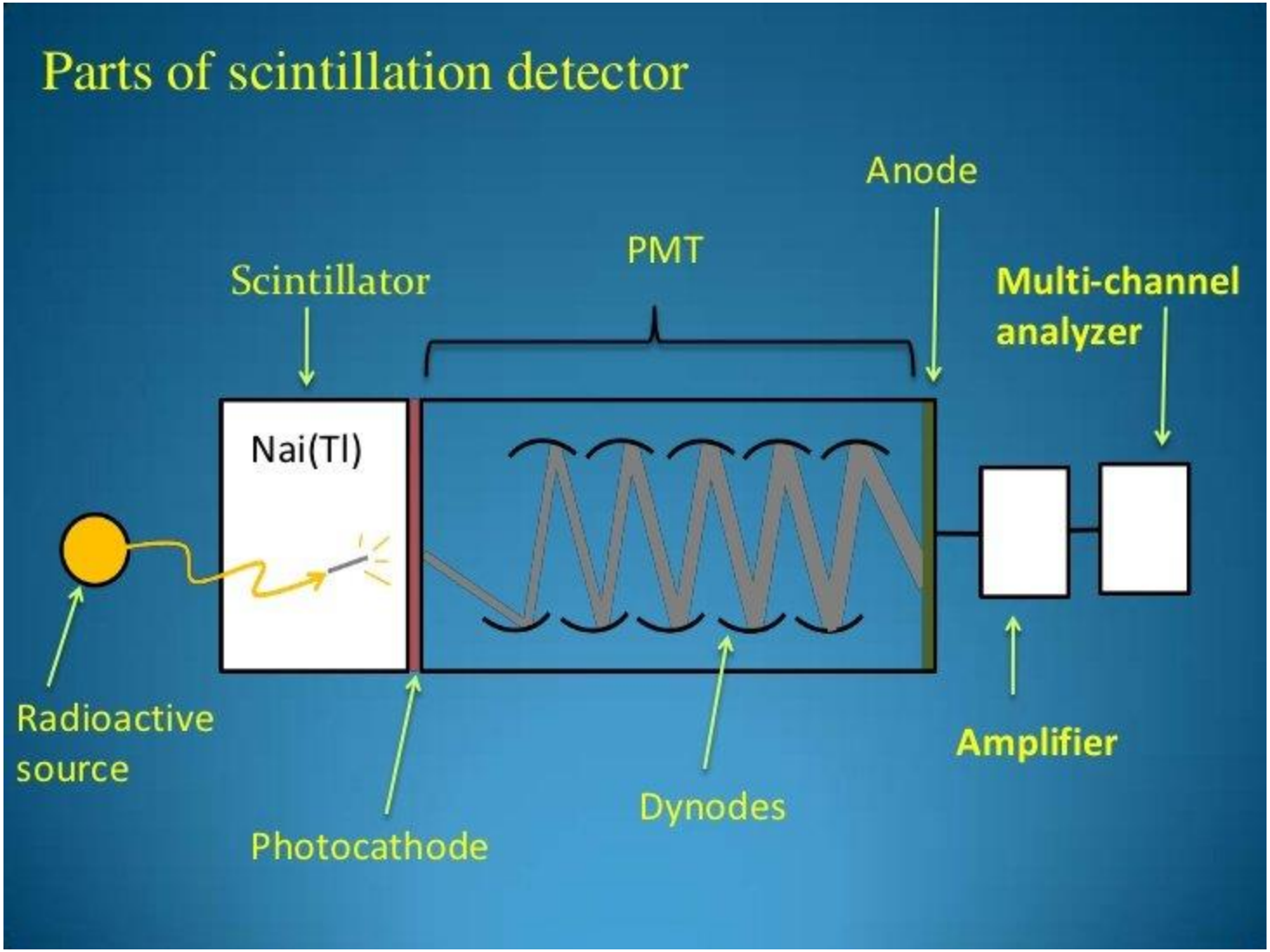
Parts of scintillation detector
Anode
PMT
Scintillator
Multi-channel analyzer
Nai(Tl)
Radioactive source
Photocathode
Dynodes
Amplifier

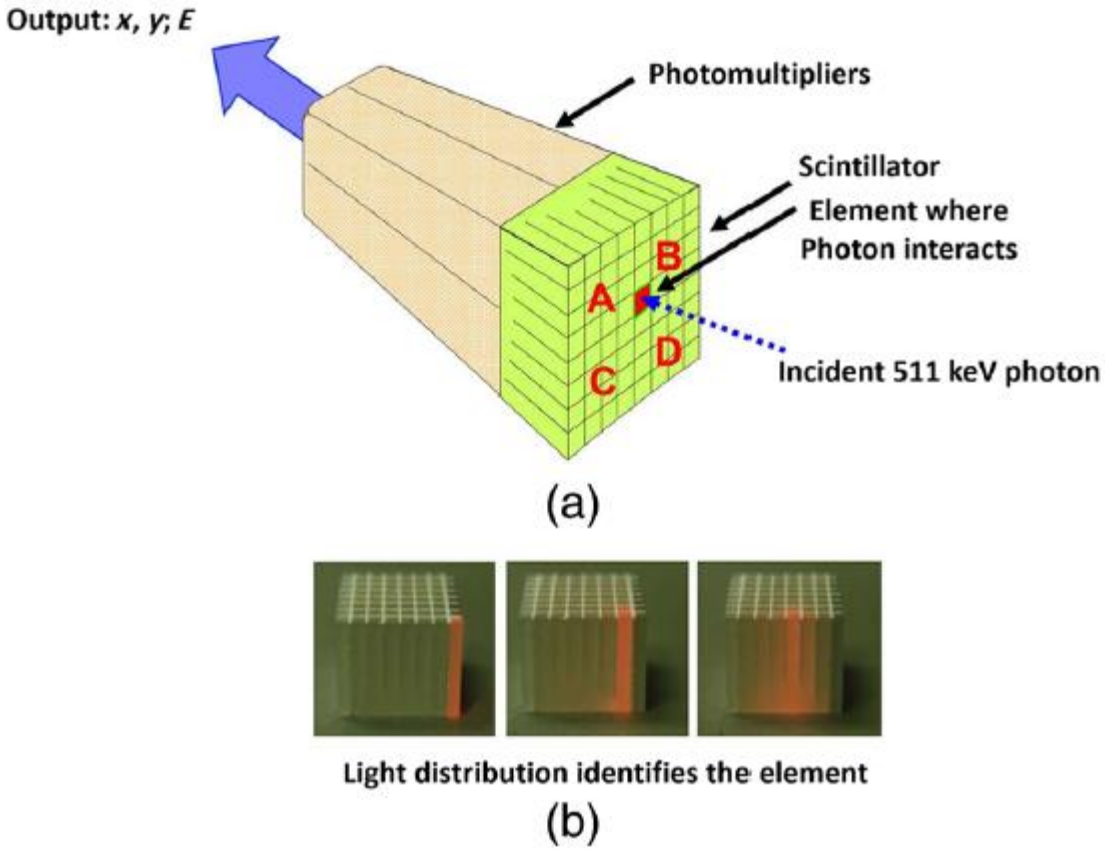

Fig. 4 (a) The block detector concept invented by Casey and Nutt in 1985. The incident annihilation photon is converted to light in the scintillator and the sharing of light (b) between the four photomultiplier tubes identifies the scintillator element and localizes the incident photon. The output from the block detector is the coordinates of the element (x, y) and the energy (E) of the photon obtained by summing the light produced in the scintillator.

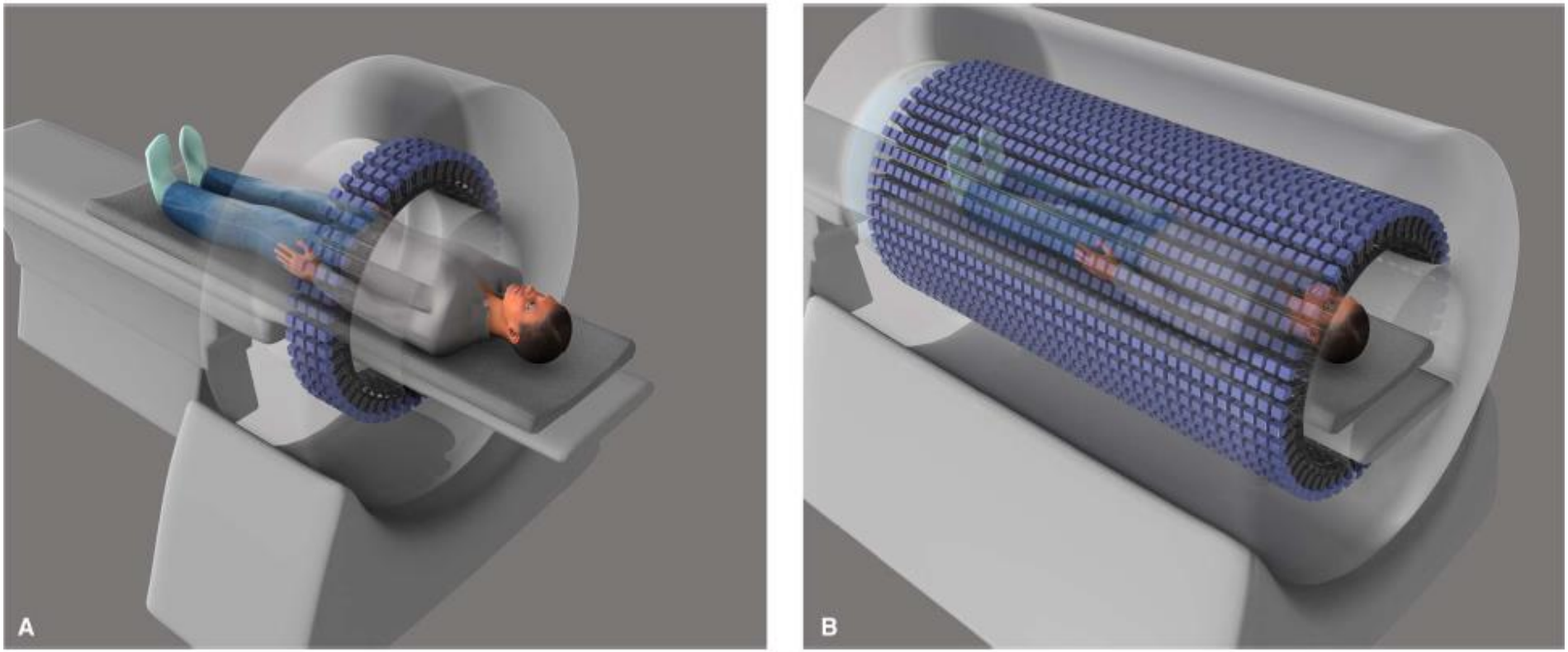

Fig. 1. Seeing into our future. Illustration depicting (**A**) a conventional PET scanner and (**B**) total-body PET (TB-PET) scanner. An x-ray computed tomography (CT) scanner will be mounted on the front of the TB-PET gantry for anatomical coregistration to ensure optimal integration of anatomical imaging with molecular imaging.

(A)

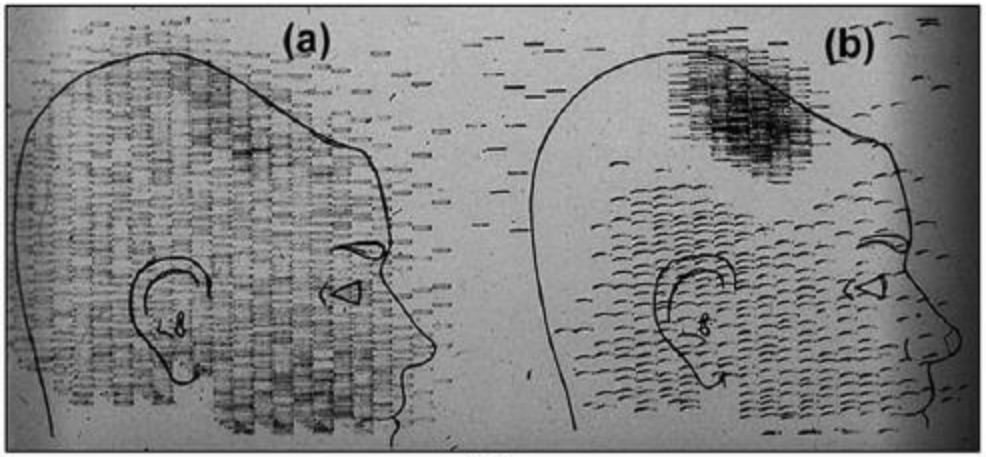

(B)

Fig 1 (A) First clinical positron imaging device developed in 1953 by Dr. Brownell (left) and Dr. Aronow (right), and (B) the coincidence and unbalance scans of patient with recurring brain tumor. The coincidence scan (a) of a patient showing recurrence of a tumor under the previous operation site, and unbalance scan (b) showing asymmetry to the left. [Reproduced from Ref. 6].

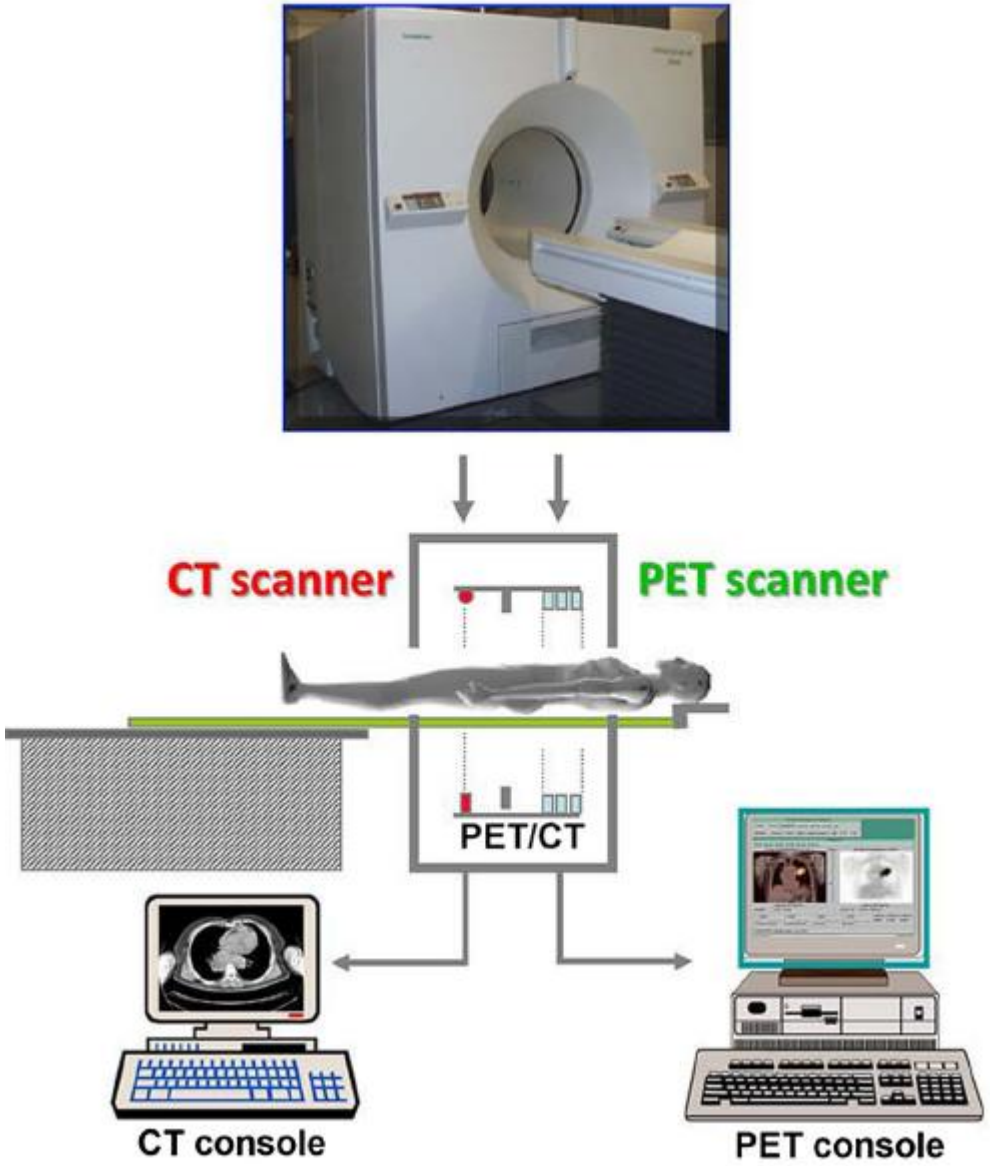

Fig. 11 The first PET/CT scanner design (a) combining a spiral CT scanner with a rotating ART PET scanner mounted on the same support as the CT. The CT images are acquired first by moving the bed continuously through the scanner, whereas the PET images are acquired by discrete steps of the bed as shown in Fig. 7. The fused images (b) of CT and PET are displayed on the screen for reading by the attending radiologist.

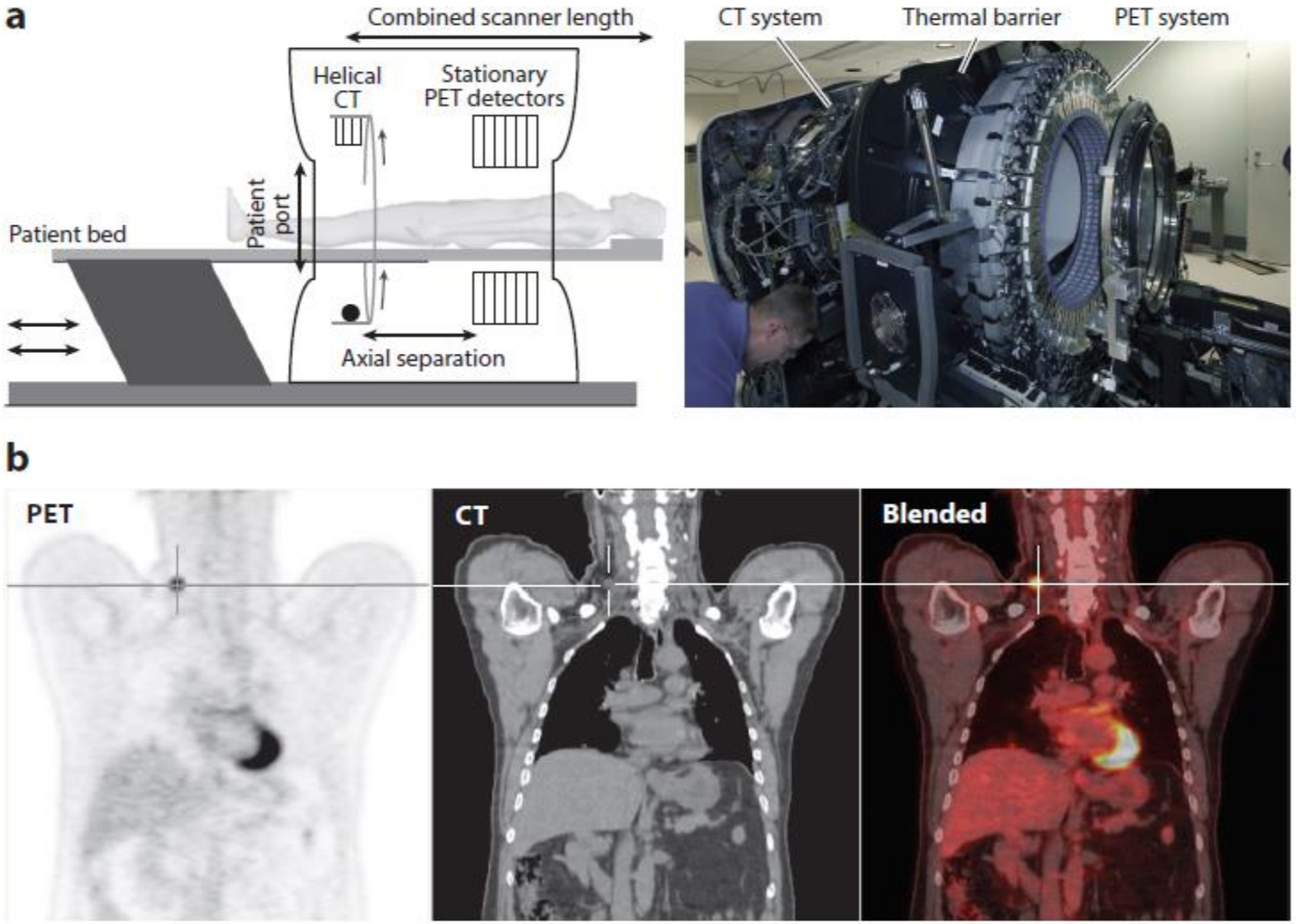

Figure 9

(*a*) Schematic and photograph of a combined positron emission tomography and computed tomography (PET–CT) scanner used for clinical applications. Although the concept of aligning in tandem a CT scanner and a PET scanner is simple, the technical and practical complexities pose challenges that range from the footprint size of the resulting system to the spatial and temporal alignment of the resulting data sets. (*b*, *left to right*) The coronal view of a clinical ^{18}FDG PET scan clearly shows a recurrent thyroid cancer tumor (*crosshair*), the CT image shows detailed anatomy in which the tumor is hardly distinguishable, and the blended image shows the precise anatomical localization (from the CT image) of the active tumor (from the PET image).

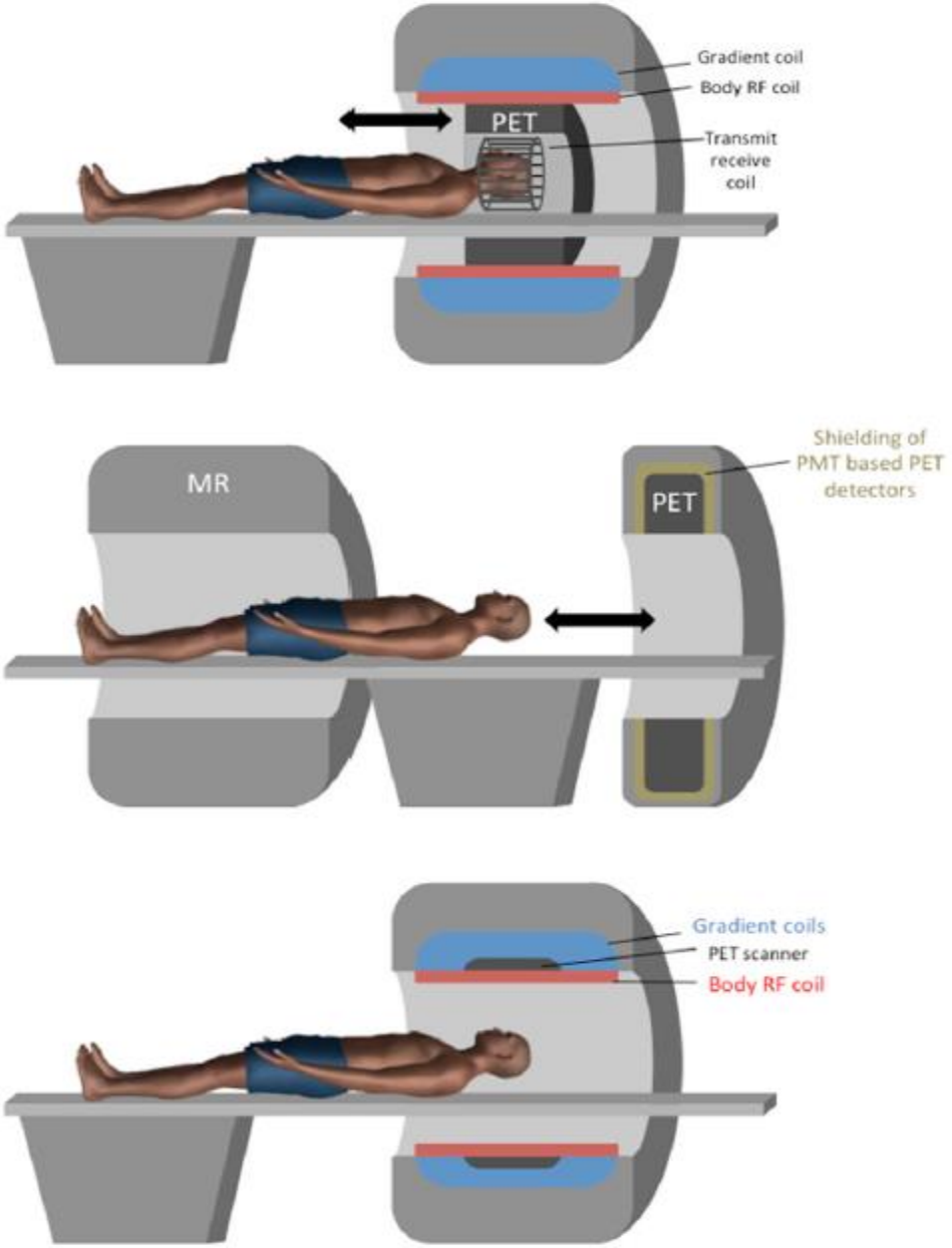

Figure 10. Three concepts for integration of PET and MRI: a brain PET scanner inserted in a whole body MRI (top), a sequential PET MRI scanner for whole body imaging (middle) and a fully integrated simultaneous PET MRI scanner for patient imaging (bottom).

Fig. 13 The combined PET/MR scanner (Siemens Healthineers) with simultaneous MR and PET imaging capability.

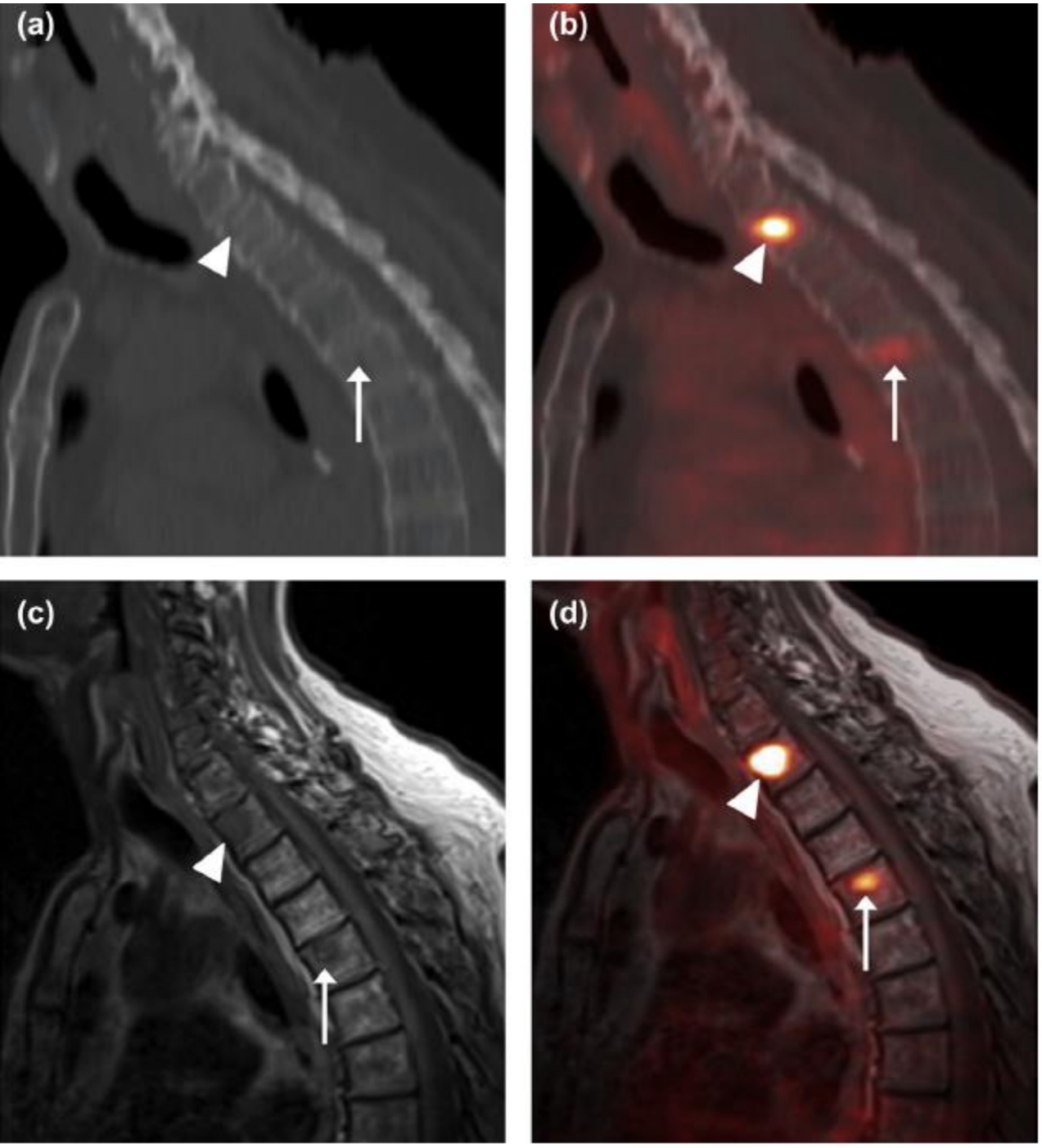

Figure 2. 69-year-old man with known metastatic papillary thyroid carcinoma presented for restaging. Sagittal computed tomography (CT) images **(a)** revealed a subtle lytic lesion within the T2 vertebral body (*arrow head*) but a normal appearance of the T5 vertebral body (*arrow*). Sagittal CT images with 2-deoxy-2-[^{18}F]fluoro-D-glucose-positron emission tomography (FDG-PET) fusion **(b)** demonstrated an FDG-avid focus in the T2 (*arrowhead*) vertebral body highly suspicious for metastatic disease. In contrast, a focus of more subtly increased FDG uptake in the T5 vertebral body (*arrow*) without a CT correlate was felt to be indeterminate, as both metastatic disease and degenerative disease could conceivably produce this appearance. Sagittal T1-weighted images (T1WIs) **(c)** from subsequent PET/magnetic resonance imaging (MRI) showed clear evidence of marrow replacement in the T2 (*arrowhead*) and T5 (*arrow*) vertebral bodies. Corresponding foci of FDG avidity on sagittal T1WIs with FDG-PET fusion **(d)** strongly supported the presence of metastases at both sites. These images show an example of the improved anatomic delineation of malignant osseous disease with PET/MRI relative to PET/CT, as well as the power of PET/MRI to distinguish osseous malignancy from degenerative remodeling.

References

[1] Unterrainer, M. et al. (2020). Recent advances of PET imafing in clinical radiation oncology. *Radiation Oncology, 15*, 88.

[2] Rosenkrantz, A. B. et al. (2016). Current status of hybrid PET/MRI in oncologic imaging. *American Journal of Roentgenology*, *Vol. 206. No. 1*, 162-172.

[3] Berg, E. and Cherry, S. R. (2018). Innovations in instrumentation for positron emission tomography. *Seminars in Nuclear Medicine*, DOI: 10.1053/j.semnuclmed.2018.02.006.

[4] Jones, T. and Townsend, D. (2017). History and future technical innovation in positron emission tomography. *Journal of Medical Imaging*, *Vol. 4. No. 1*, 011013.

[5] Vaquero, J. J. and Kinahan, P. (2015). Positron emission tomography: current challenges and opportunities for technological advances in clinical and preclinical imaging systems. *Annual review of Biomedical Engineering*, *17*, 385-414.

[6] Cherry, Simon R. et al. (2017). Total-body imaging: transforming the role of positron emission tomography. *Science Translational Medicine, 9*, 381.

[7] Watanabe, M. et al. (2017). Performance evolution of a high-resolution brain PET scanner using four-layer MPPC DOI detectors. *Physics in Medicine and Biology, 62,* 7148-7166.

[8] Gong, K. et al. (2016). Designing a compact high performance brain PET scanner-simulaton study. *Physics in Medicine and Biology, 61,* 3681-3697.

[9] Tashima, H. and Yamaya, T. (2016). Proposed helmet PET geometries with add-on detectors for high sensitivity brain imaging. *Physics in Medicine and Biology, 61,* 7205-7220.

[10] Ehman, E. C. (2017). PET/MRI: where might it replace PET/CT. *Journal of Magnetic Resonance Imaging. Vol. 46. No. 5*, 1247-1262.

[11] Vandenberghe, S. and . Marsden, P. K. (2015). PET-MRI: a review of challenges and solutions in development of integrated multimodality imaging. *Physics in Medicine and Biology*, 60, R115-R154.

[12] Spick. C. et al. (2016). F-FDG PET/CT and PET/MRI perform equally well in cancer: evidence from studies on more than 2,300 patients. *Journal of Nuclear Medicine*, 57, 1-11.

[13] Hsu, D. F. C. et al. (2017). Studies of a next generation silicon-photomultiplier-based time- of-flight PET/CT system. *Journal of Nuclear Medicine, 58,* 1511-1518.

[14] Jagust, W. (2018). Imaging the evolution and pathophysiology of Alzheimer disease. *Nature Reviews Neuroscience, 19*, 687-700.

[15] Bauer, C. E. et al. (2016). Concept of an upright wearable positron emission tomography imager in humans. *Brain Behavior, 6*, e00530.